Defects in nanocrystalline Nb films: Effect of sputtering temperature

J. Čížek [a,*], O. Melikhova [a], I. Procházka [a], G. Brauer [b], W. Anwand [b], A. Mücklich [b], R. Kirchheim [c], A. Pundt [c]

[a] Department of Low-Temperature Physics, Faculty of Mathematics and Physics,
Charles University, V Holešovičkách 2, CZ-180 00, Prague 8, Czech Republic
[b] Institut für Ionenstrahlphysik und Materialforschung, Forschungszentrum Rossendorf, Dresden, Germany
[c] Institut für Materialphysik, Universität Göttingen, Germany

Abstract

Thin niobium (Nb) films (thickness 350–400 nm) were prepared on (1 0 0)Si substrate in a UHV chamber using the cathode beam sputtering. The sputtering temperature T_s was varied from 40 up to 500 °C and the influence of the sputtering temperature on the microstructure of thin Nb films was investigated. Defect studies of the thin Nb films sputtered at various temperatures were performed by slow positron implantation spectroscopy (SPIS) with measurement of the Doppler broadening of the annihilation line. SPIS was combined with transmission electron microscopy (TEM) and X-ray diffraction (XRD). We have found that the films sputtered at $T_s = 40$ °C exhibit elongated, column-like nanocrystalline grains. No significant increase of grain size with T_s (up to 500 °C) was observed by TEM. The thin Nb films sputtered at $T_s = 40$ °C contain a high density of defects. It is demonstrated by shortened positron diffusion length and a high value of the S parameter for Nb layer compared to the well-annealed (defect-free) bulk Nb reference sample. A drastic decrease of defect density was found in the films sputtered at $T_s \geq 300$ °C. It is reflected by a significant increase of the positron diffusion length and a decrease of the S parameter for the Nb layer. The defect density in the Nb layer is, however, still substantially higher than in the well-annealed reference bulk Nb sample. Moreover, there is a layer at the interface between the Nb film and the substrate with very high density of defects comparable to that in the films sputtered at $T_s < 300$ °C. All the Nb films studied exhibit a strong (1 1 0) texture. The films sputtered at $T_s < 300$ °C are characterized by a compressive macroscopic in-plane stress due to lattice mismatch between the film and the substrate. Relaxation of the in-plane stress was observed in the films sputtered at $T_s \geq 300$ °C. The width of the XRD profiles of the films sputtered at $T_s \geq 300$ °C is significantly smaller compared to the films sputtered at lower temperatures. This is most probably due to a lower defect density which results in reduced microstrains in the films sputtered at higher temperatures.
© 2005 Elsevier B.V. All rights reserved.

Keywords: Niobium films; Cathode beam sputtering; Slow positron implantation spectroscopy; X-ray diffraction

* Corresponding author. Tel.: +420 2 2191 2788; fax: +420 2 2191 2567.
E-mail address: jcizek@mbox.troja.mff.cuni.cz (J. Čížek).

1. Introduction

The growth mode of thin films prepared by sputtering is influenced by the sputtering rate (i.e. the number of atoms which hit the substrate per unit of time) and by the sputtering temperature T_s (the temperature of substrate). Higher T_s leads to an enhanced mobility of the sputtered atoms in the substrate plane and long-range diffusion processes start to play an important role in the growth of the film. The effect of T_s is clearly visible on niobium (Nb) films [1]: polycrystalline Nb films are produced by sputtering at room temperature, while a high sputtering temperature $T_s = 850\,°C$ results in a formation of epitaxial films. One can expect that the sputtering temperature influences not only the grain size but also the density and type of lattice defects in thin films. Thus, it is highly desirable to perform defect studies of thin films sputtered at various T_s. The characterization of thin films prepared by sputtering is usually performed by X-ray diffraction (XRD). The shape of the diffraction profile is influenced by grain size as well as microstrains which could originate, e.g. from dislocations. On the other hand, point defects (e.g. vacancies) can only hardly be detected by XRD. For these reasons positron annihilation spectroscopy (PAS) is very useful for defect studies of thin Nb films because it exhibits a high sensitivity to open-volume point defects like vacancies, vacancy clusters, etc. [2]. Hence, XRD and PAS represent in certain way complementary techniques and their combination in investigations of thin films is very efficient.

In the present work we investigated the microstructure of thin Nb films prepared at various T_s. Defect studies of the films were performed by slow positron implantation spectroscopy (SPIS) with measurement of the Doppler broadening of the annihilation line. The SPIS investigations were combined with XRD studies and direct observation of the microstructure by transmission electron microscopy (TEM). The purpose of this work was to clarify the influence of T_s on the microstructure of thin Nb films.

2. Experimental details

Thin Nb films were prepared on polished (1 0 0)Si substrates in an UHV chamber using cathode beam

sputtering at sputtering temperatures $T_s = 40$, 100, 200, 300, 400 and 500 °C. The desired T_s was stabilized during sputtering within $\pm 1\,°C$. In addition, one Nb film was sputtered at $T_s = 40\,°C$ and subsequently annealed at 500 °C for 1 h in UHV (10^{-10} mbar). The surface of all samples was covered with a 20 nm thick Pd cap in order to prevent oxidation. The thickness of the films was measured by TEM and found to lie in the range 350–400 nm for various films. The SPIS studies were performed at a magnetically guided positron beam "SPONSOR" [3] with positron energies adjustable from 0.03 to 36 keV. Energy spectra of annihilation gamma rays were measured by a Ge detector with an energy resolution of 1.09 ± 0.01 keV at 511 keV. The texture measurements were carried out on a four-axis Philips X'pert MPD diffractometer using Co Kα radiation. XRD measurements of lattice constants were performed at Hasylab (DESY) using synchrotron radiation with wavelength $\lambda = 1.13\,Å$. The inter-planar distance was measured in the out-of-plane direction (i.e. in the direction perpendicular to the film surface, which corresponds to $\psi = 0°$) and in the directions tilted by $\psi = 45°$ and 60° with respect to normal to the surface. In such a way, we obtained information about stress in the studied films. Diffraction profiles were fitted by the Pearson VII function. TEM studies were performed with a Philips CM300SuperTWIN microscope operating at 300 kV. Thin foils for cross sectional TEM were produced by conventional preparation using Gatan precision ion polishing system (PIPS).

3. Results and discussion

A bright field TEM image of the film sputtered at $T_s = 40\,°C$ is shown in Fig. 1a. The film exhibits elongated "column-like" grains. The width of columns does not exceed 100 nm. Typically it lies around 50 nm. A high resolution image of a column is shown in Fig. 1b. The columns are divided horizontally (i.e. in direction perpendicular to film-growing direction) into two "generations" of sub-columns. The "first generation" sub-columns are situated close to the Si substrate, while the "second generation" sub-columns are situated close to the film surface. A bright field TEM image of the film sputtered at $T_s = 500\,°C$ is shown in Fig. 2a. From comparison of Figs. 1a and 2a
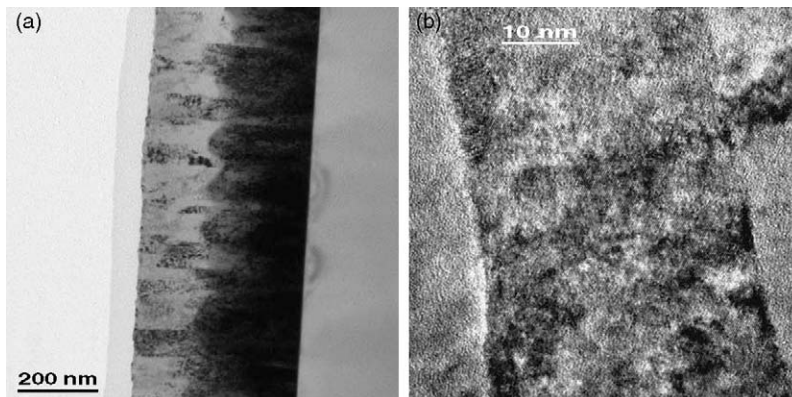
Fig. 1. (a) A bright field TEM image of the film sputtered at $T_s = 40\ ^\circ$C and (b) a high resolution image of a single column-like grain in the film.

it is clear that there is basically no difference detectable by TEM between the film sputtered at 40 °C and at 500 °C. A high resolution TEM image of the film sputtered at 500 °C is shown in Fig. 2b.

A strong 1 1 0 texture was found in all the studied films. Most of grains are oriented so that the {1 1 0} planes are situated parallel with the film surface. However, the lateral orientation of grains is random. The texture becomes better developed at higher T_s.

In order to illustrate the effect of T_s on the X-ray diffraction pattern, the XRD profiles corresponding to (1 1 0)Nb reflection for selected films sputtered at various T_s are shown in Fig. 3a and b. The profiles shown in Fig. 3a were measured in the direction $\psi = 0^\circ$, i.e. the scattering vector is perpendicular to the film surface. The XRD profiles plotted in Fig. 3b were measured on tilted sample at position $\psi = 60^\circ$, i.e. the angle included by the scattering vector and the

normal to the film surface is 60°. Thus, the inter-planar distance determined from position of the reflections in Fig. 3a and b, respectively, correspond to the distance between the {1 1 0} planes in the out-of-plane direction and in the direction tilted by 60° with respect to normal to the film surface. The distance $d_{1\ 1\ 0}$ between the {1 1 0} planes in bulk Nb is indicated in Fig. 3a and b by a dashed line. One can see from Fig. 3a that $d_{1\ 1\ 0}$ in the direction $\psi = 0^\circ$ is higher than that for bulk Nb in all the films studied. On the other hand, $d_{1\ 1\ 0}$ in the direction $\psi = 60^\circ$ is slightly smaller than in bulk Nb. It indicates an existence of compressive in-plane stresses in the films caused by a lattice mismatch between the film and the Si substrate. The magnitude of the compressive stress decreases with increasing T_s, which is reflected by a shift of the reflections towards the positions for bulk Nb. One can see from Fig. 3a that there is a significant
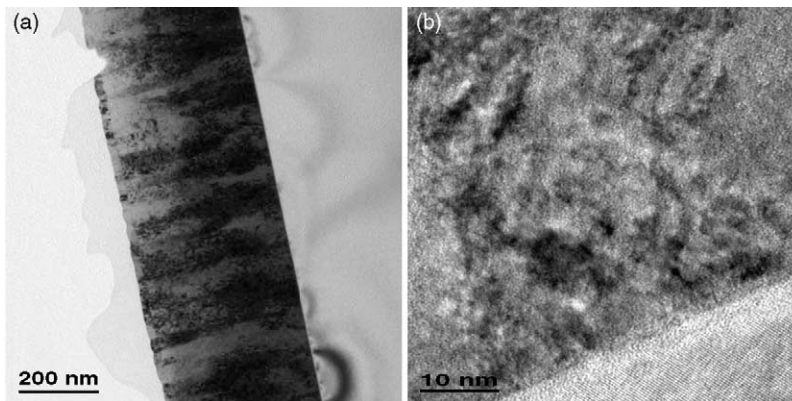

Fig. 2. (a) A bright field TEM image of the film sputtered at $T_s = 500\ ^\circ$C and (b) a high resolution image of a single column-like grain in the film.
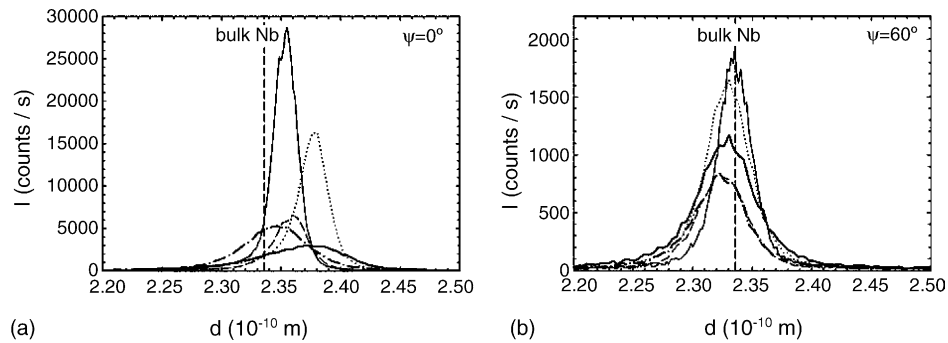
Fig. 3. XRD profiles for selected films measured at position (a) $\psi = 0°$ and (b) $\psi = 60°$. Thicker solid line, $T_s = 40$ °C; dotted line, $T_s = 200$ °C; dashed line, $T_s = 300$ °C; thin solid line, $T_s = 500$ °C; dash-dotted line, $T_s = 40$ °C with subsequent annealing at 500 °C for 1 h. The $d_{1\,1\,0}$ inter-planar distance in the bulk Nb is indicated by the vertical-dashed lines.

change of the position of the (1 1 0) reflection for $T_s \geq 300$ °C. Thus, starting from $T_s = 300$ °C the compressive stresses in the films are partially relaxed. Not only the position but also the width of the reflections depends strongly on T_s. The broadening of XRD profiles is caused either by small grain size or by microstrains induced by local elastic field of certain defects, e.g. misfit dislocations. From Fig. 3a it is clear that the sample prepared at $T_s = 500$ °C exhibits the narrowest XRD profile. On the other hand, the highest width of the XRD profile was found on the film sputtered at $T_s = 40$ °C. As no difference in grain size between these two samples has been observed by TEM, we conclude that the narrowing of XRD profile for the film sputtered at $T_s = 500$ °C is due to a decrease of defect density. The increase of T_s from 40 to 200 °C leads to a decrease of width of XRD profiles caused by a decrease of defect density. However, the relaxation of compressive stresses at $T_s = 300$ °C

which leads to a shift of the peak position is accompanied by an increase of the width of the reflection, see Fig. 3a. It could be due to introduction of misfit dislocations which accommodate the stresses caused by the lattice mismatch. Further increase of T_s from 300 to 500 °C leads again to a significant narrowing of XRD profiles due to decrease of defect concentration in the film. Note that the film sputtered at $T_s = 40$ °C and subjected to subsequent annealing at 500 °C is characterized by relaxation of the stresses, i.e. a shift of the peak position towards that for bulk Nb, however, the width of the profile remains large. It indicates that defect density in this film is comparable with the film sputtered at $T_s = 40$ °C.

The reflection measured at $\psi = 0°$ for the film sputtered at $T_s = 40$ °C is asymmetric. It can be well seen in Fig. 4a where it is plotted in a finer scale. The shape of the profile indicates that it is a superposition
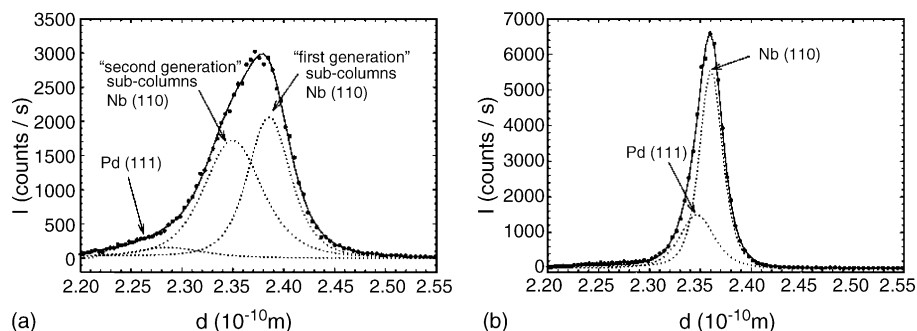

Fig. 4. (a) XRD profile for the film sputtered at $T_s = 40$ °C, measured in position $\psi = 0°$ and (b) XRD profile for the film sputtered at $T_s = 300$ °C, measured in position $\psi = 0°$. The profile is a superposition of several reflections shown by the dotted lines.

of several reflections, namely: (i) the (1 1 0) reflection from the "first generation" sub-columns in Nb layer, (ii) the (1 1 0) reflection from the "second generation" sub-columns in Nb layer and (iii) a weak and broad (1 1 1) reflection from the Pd cap. Note that it is not possible to fit the XRD profile properly without the assumption of different distances $d_{1\,1\,0}$ in the "first generation" and in the "second generation" sub-columns. The same result was obtained on a thicker (1.1 μm) Nb film sputtered under the same conditions (see ref. [4] for more detailed discussion). The asymmetry of XRD profiles disappears at $T_s \geq 300\ ^\circ$C °C and the profiles are then well-fitted by a single (1 1 0) reflection from the Nb layer and the reflection from Pd cap. As an example, the XRD profile for the film sputtered at $T_s = 300\ ^\circ$C is shown in Fig. 3b.

Additionally, the inter-planar distance $d_{1\,1\,0}$ (Nb(1 1 0) reflection) in the direction $\psi = 60^\circ$ and the distance $d_{2\,0\,0}$ (Nb(2 0 0) reflection) in the direction $\psi = 45^\circ$ were measured. Both the $d_{1\,1\,0}$ and $d_{2\,0\,0}$ distances for the two generations of sub-columns lie in these directions too close to each other to separate their reflections in XRD spectrum.

The lattice constants a calculated from the inter-planar distance in the directions $\psi = 0^\circ$, 45° and 60° are plotted in Fig. 5a as a function of T_s. The lattice constant for bulk Nb [5] is shown in the figure by a dashed line. Below $T_s = 300\ ^\circ$C, the inter-planar distance in the two "generations" of sub-columns differs in the direction $\psi = 0^\circ$. The "first generation" sub-columns exhibit a higher $d_{1\,1\,0}$ in this direction than the "second

generation" sub-columns. On the other hand, above $T_s = 300\ ^\circ$C, there is no significant difference between $d_{1\,1\,0}$ in both "generations" of sub-columns and there is only a single value of a for $\psi = 0^\circ$. One can see in Fig. 5a that a in the direction $\psi = 0^\circ$ lies significantly above that for bulk Nb. A progressive decrease of a takes place from $T_s = 40–200\ ^\circ$C, while at higher $T_s > 300\ ^\circ$C it becomes approximately constant. The values of a in the direction $\psi = 60^\circ$ are lower than in the bulk Nb. It testifies the existence of compressive stresses in the in-plane direction in all the films studied. Only moderate changes of a with T_s can be seen in the directions $\psi = 45^\circ$ and 60°. The main feature is a decrease of a at $T_s = 300\ ^\circ$C. Annealing of the film at $500\ ^\circ$C after sputtering ($T_s = 40\ ^\circ$C) leads to a substantial decrease of a, see Fig. 5a, which becomes even lower than that for the film sputtered at $T_s = 500\ ^\circ$C. Thus, annealing of the as-sputtered films seems to be an effective way how to relax the compressive stresses.

The dependence of the S parameter on positron energy E for selected Nb films is plotted in Fig. 5b. A local minimum of S at $E = 1$ keV is due to positron annihilations in the Pd cup. It was confirmed by measurement of a reference Pd film. Subsequent increase of S is caused by an increasing fraction of positrons annihilating inside the Nb layer. In the energy range from 5 to 7 keV, the contribution of positron annihilations inside the Nb layer is maximal and S exhibits a plateau-like behavior. At higher energies, positrons start to penetrate into the Si
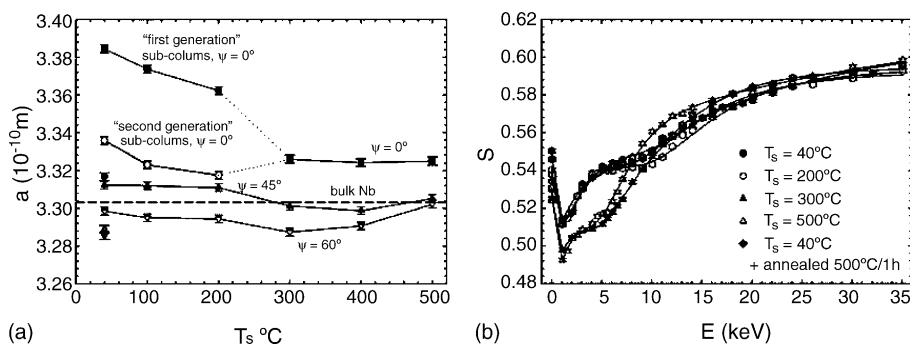

Fig. 5. (a) The lattice constant a determined from inter-planar distances in various directions as a function of T_s. Full circles, direction $\psi = 0^\circ$, "first generation" sub-columns; open circles, direction $\psi = 0^\circ$, "second generation" sub-columns; full squares, direction $\psi = 0^\circ$, both "generations" of sub-columns ($T_s \geq 300\ ^\circ$C); full triangles, direction $\psi = 45^\circ$; open triangles, direction $\psi = 45^\circ$, the gray symbols corresponds to the film sputtered at $T_s = 40\ ^\circ$C and subjected to subsequent annealing at $500\ ^\circ$C; gray circle, direction $\psi = 45^\circ$; gray triangle oriented-up, $\psi = 45^\circ$; gray triangle oriented-down, $\psi = 60^\circ$ and (b) dependencies of the S parameter on positron energy E for selected films. The solid lines show the fit performed by VEPFIT.
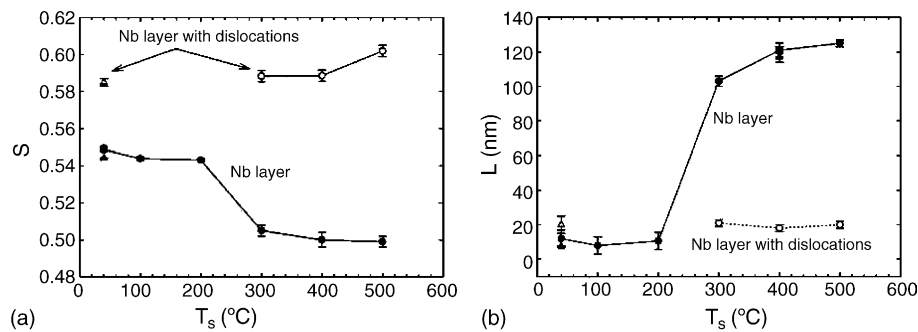
Fig. 6. Results of fit of the $S(E)$ curves (a) dependence of fitted S on T_s; full circles, S for the Nb layer; open circles, S for the layer with misfit dislocations situated close to the interface between the films and the substrate; full triangle, S for the Nb layer for the film sputtered at $T_s = 40$ °C and subjected to subsequent annealing at 500 °C; open triangle, S for the layer with misfit dislocations for the film sputtered at $T_s = 40$ °C and subjected to subsequent annealing at 500 °C and (b) dependence of positron diffusion length on T_s; full circles, Nb layer; open circles, the layer with misfit dislocations, the triangles denote the results for the film sputtered at $T_s = 40$ °C and subjected to subsequent annealing at 500 °C; full triangle, Nb layer; open triangle, the layer with misfit dislocations.

substrate which leads to further increase of S. As one can see in Fig. 5b, there is not much difference between the $S(E)$ curves for $T_s = 40$ and 200 °C as well as for the film sputtered at $T_s = 40$ °C and subjected to additional annealing at 500 °C. On the other hand, the shape of the $S(E)$ curves has changed remarkably for the film sputtered at $T_s = 300$ and 500 °C. The $S(E)$ curves were fitted by the VEPFIT software package [6] (see the solid lines in Fig. 5b). For $T_s < 300$ °C, the $S(E)$ curves were well-fitted using a three-layer model: Pd cap, Nb layer and Si substrate. However, this approach failed for the films sputtered at $T_s > 300$ °C. In order to create a model which fits satisfactorily the $S(E)$ curves for the films sputtered at higher temperatures it was necessary to assume the existence of an additional layer with a high density of defects situated close to the interface between the film and Si substrate. Such a layer could contain predominantly misfit dislocations which accumulate the lattice mismatch between the film and the substrate. The dependence of the fitted S parameter for Nb layer on T_s is plotted in Fig. 6a. For $T_s \geq 300$ °C, the S parameter for the defected layer situated close to the film interface with substrate is plotted in Fig. 6a as well. The fitted positron diffusion length L for the Nb layer (for $T_s \geq 300$ °C also for the layer with defects) is plotted in Fig. 6b as a function of T_s. The S parameter lies well above that for the reference defect-free bulk Nb at all T_s. It indicates that a significant fraction of positrons annihilate from the trapped state at defects. Clearly, there is a pronounced change of S as well as L

at $T_s = 300$ °C. The XRD studies have revealed that relaxation of the compressive stresses occurs at $T_s = 300$ °C. This process leads probably to an introduction of misfit dislocations and to the formation of the defect layer because the lattice mismatch between the film and the substrate is no more compensated by the elastic strains. Thus, a layer with high density of misfit dislocations is formed close to the interface between the film and the substrate, while the defect density in the rest of the film is reduced as indicated by a decrease of S and increase of L. One can see in Fig. 6b that the positron diffusion length in the defected layer is comparable with that in the films sputtered at $T_s < 300$ °C and it does not change with T_s. The positron diffusion length for the remaining Nb layer exhibits a moderate increase also at $T_s > 300$ °C, accompanied by a decrease of corresponding S parameter. It indicates a further reduction of the defect density in the films.

4. Conclusions

The influence of the sputtering temperature T_s (varied from 40 to 500 °C) on the microstructure of thin Nb films was studied. The films are characterized by column-like grains (width < 100 nm) and compressive in-plane stresses. It was found that the grain size is basically independent on T_s. A partial relaxation of the stresses occurs at $T_s = 300$ °C and is demonstrated by a shift of XRD reflections. SPIS

studies have shown that the stress relaxation is accompanied by an introduction of misfit dislocations in a layer situated close to the interface between the film and the substrate, while the defect density in the remaining part of the film decreases.

Acknowledgements

References

[1] U. Laudahn, A. Pundt, M. Bicker, U.V. Hülsen, U. Geyer, T. Wagner, R. Kirchheim, J. Alloys Compd. 293–295 (1999) 490.

[2] P. Hautojärvi, C. Corbel, in: A. Dupasquier, A.P. Mills, Jr. (Eds.), Positron Spectroscopy of Solids, IOS, Amsterdam, 1995, p. 491.

[3] W. Anwand, H.-R. Kissener, G. Brauer, Acta Phys. Pol. A 88 (1995) 7.

[4] J. Čížek, I. Procházka, G. Brauer, W. Anwand, A. Mücklich, R. Kirchheim, A. Pundt, this volume.

[5] ICDD (International Centrum for Diffraction Data) powder diffraction pattern database PDF-2.

[6] A. van Ween, H. Schut, M. Clement, J. de Nijs, A. Kruseman, M. Ijpma, Appl. Surf. Sci. 85 (1995) 216.